

ARTICLE TEMPLATE

Environmental and economic benefits of building retrofit measures for the residential sector by utilising sensor data and advanced calibrated models

Fabiano Pallonetto^{a,b} and Mattia De Rosa^{a,c} and Donal P. Finn^{a,c}

^aUCD Energy Institute; ^bSchool of Electric and Electronic Engineering; ^cSchool of Mechanical and Materials Engineering, University College Dublin, Belfield, Dublin 04 V1W8, Ireland

ARTICLE HISTORY

Compiled August 11, 2020

ABSTRACT

The present paper investigates the energy savings associated with the implementation of retrofitting measures on Irish residential buildings. A detached residential dwelling, representative of approximately 40% of the residential stock in Ireland, was selected as experimental test bed. The building was progressively retrofitted to an all electric dwelling. Retrofit measures included the installation of a photovoltaic array, a geothermal heat pump, an electric vehicle charging point, along with building fabric upgrades. The building was equipped with a home area network with more than 30 sensors with 15 minute monitoring resolution. The experimental data collected during the experimental campaign aided the comprehensive calibration of an EnergyPlus model. This model was used to investigate the effectiveness of the implemented retrofit measures in terms of energy savings and CO₂ reductions. Real-time data from the Irish power system operator was used to calculate the building carbon footprint for different levels of renewable energy penetration to the national grid. Results show that the all-electric retrofitted building can achieve energy savings of up to 45%, with CO₂ reductions of approximately 29%, compared to the pre-retrofitted building. Implementing the retrofit measures at scale could potentially lead to carbon emission reductions up to 14% for rural areas in Ireland.

KEYWORDS

building energy model; calibration; decarbonisation; renewable energy; electric vehicles; geothermal heat pump; solar energy.

1. Introduction

Following the ratification of the Paris agreement, member countries of the European Union have set ambitious targets of 40% carbon emissions reduction by 2030 and 60% by 2040 (Rogelj et al., 2016). In this context, the building sector plays a critical role in meeting these targets, being responsible for more than 40% of the overall energy demand worldwide (Carragher, De Rosa, Kathirgamanathan, & Finn, 2019), with expected increasing trends over the coming decades (Szalay & Csoknyai, 2014). For instance, heating and cooling energy consumption accounts for about 36% of all carbon emissions in Europe (D'Ettorre, De Rosa, Conti, Testi, & Finn, 2019). Therefore,

a substantial decarbonisation can be achieved by implementing appropriate energy policies and regulations for the building sector. The Energy Performance of Building Directive (EPBD) (European Union, 2018) and the Energy Efficiency Directive (EED) (European Union, 2012) represent the main legislative instruments established by the European Union (EU) to establish minimum energy performance standards for new buildings and to foster the implementation of retrofitting measures in old buildings. Furthermore, new legislation has been introduced by the EU to support the use of smart technologies - such as building home automation, the deployment of smart grid infrastructure, the diffusion of smart appliances and Energy Management System (EMS) integration - which can contribute to the optimisation of building energy consumption for the more rational use of energy (Vázquez-Canteli & Nagy, 2019).

Most of the efforts to date have been put into improving the energy efficiency of new buildings (Thomsen et al., 2016) in order to meet the net zero-energy buildings (nZEB) criterion, as required by the EPBD (European Union, 2018). On the other hand, only around 1% of the existing building stock is renovated in Europe on an annual basis (European Union, 2016), despite the significant reduction of energy consumption that could be achieved by improving their energy performance. More recently, several retrofitting strategies have been developed and investigated as a function of the building characteristics, climate conditions, policy and financial environments (Leal, Granadeiro, Azevedo, & Boemi, 2015). Structural interventions - such as, improved insulation materials (Castaldo et al., 2015), more efficient equipment and renewable-based energy and associated storage systems (Leal et al., 2015) - have been proposed and tested. However, barriers such as the large investment required, architectural constraints, uncertainties over human behaviour change and lack of knowledge among stakeholders about technical improvements and investment opportunities continue to limit the widespread adoption of retrofitting interventions (Ma, Cooper, Daly, & Ledo, 2012).

Generally, Rey (2004) defines the idea of a retrofitting strategy as *"a set of interventions, dictated by a coherent architectural attitude and technically optimised, in particular through a full coordination of the interventions on the sheathing surfaces and the technical installations"*, which can have many different goals, i.e, increasing the building value, meeting new mandatory standards, etc. The process for retrofitting existing buildings involves five major phases (Ma et al., 2012): (i) project set up and pre-retrofit survey, (ii) energy auditing and performance assessment, (iii) identification of retrofit options, (iv) site implementation and commissioning, and (v) validation and verification. Many factors may influence the success of a building retrofitting process, which includes policy and regulations, overall budget, technologies, information and data availability, uncertainties over human factors, etc. A customised cost-optimal solution, which harmonises the two conflicting targets of minimising the energy consumption while maximising the economic benefit, needs to be found (Mauro, Hamdy, Vanoli, Bianco, & Hensen, 2015).

In this context, the implementation and assessment of retrofitting measures require to accurately estimate the impact of building retrofit measures and control equipment, such as EMS systems. The availability of increasing computational power allows simulation software models to be more detailed and accurate (Atam, 2017). However, developing an integrated model of building thermal behaviour is still a complex task that cannot be fully automated yet. The representation of a building model is composed of multiple physical models that, during the simulation, exchange data and provide an estimate of the energy consumption for each time step (Oller, Rodríguez, González, Fariña, & Álvarez, 2018). The level of detail required to describe a building

is highly variable, since it depends on the specific application analysed. New generations of building simulation software can take into account weather data, building thermal features, occupancy profiles, solar irradiation and the electric and thermodynamic characteristics of all system components.

Building simulation software has been historically used both for long-term analysis, such as seasonal schedules, as well as for analysis of short-term daily load operations (Haves, Salsbury, Claridge, & Liu, 2001). However, it has become a useful tool to identify critical issues in day-to-day building operations as well and it can support both design and retrofit interventions (Pallonetto, Mangina, Finn, Wang, & Wang, 2014). Moreover, coupling building energy simulation models with specific building archetypes (Pallonetto, Mangina, Milano, & Finn, 2019), determined by means of clustering and/or classification techniques and representative of the national building stock, has the potential to facilitate the assessment of energy savings and carbon emissions reduction potential at a wider scale (Goy, Ashouri, Maréchal, & Finn, 2017). The most utilised approach for building classification is based on predefined categories, such as age and building typologies. Generally, the building stock can be divided into residential and commercial buildings and census data or building surveys can be used to collect relevant information to characterise the building stock at a country level (Mata, Kalagasidis, & Johnsson, 2014). Once the representative archetypes are determined, specific building simulation models can be developed and calibrated to create tools for energy consumption assessment and forecasting.

The calibration of Building Energy Models (BEM) is essential to produce realistic results and it can provide guidelines for the implementation of retrofit measures (Allesina, Mussatti, Ferrari, & Muscio, 2018). Many relevant factors affecting the energy consumption of residential buildings are not captured during traditional energy audits or surveys (Glasgo, Hendrickson, & Azevedo, 2017). Therefore, the importance of accurate sensor data over the life cycle of a building is widely recognised as essential for accurate model calibration and the assessment of retrofit measures (Fabrizio & Monetti, 2015). Comprehensive investigations based on complete, ground-truth input data and metered end-user consumption are still needed to better understand the causes of calibration errors, to improve the modelling process and to assess the benefit of accurate building models during the different phases of the building life, especially when retrofit measures are implemented at scale (Li, Tian, Lu, & Fu, 2018).

Notwithstanding, the calibration of a building model can present several challenges depending on the model complexity, since it requires an extensive experimental phase to equip the building with sensors and to collect data at sub-hourly resolution (Fabrizio & Monetti, 2015). For instance, Clauß, Vogler-Finck, and Georges (2018) calibrated a building model based on a reference period of four months, reaching average errors below 5%. However, the dynamics of the indoor thermal environment, which are paramount for describing the short-term building behaviour (De Rosa, Bianco, Scarpa, & Tagliafico, 2016), were measured for two months only, equivalent to half of the reference period. Moreover, the analysis was performed on an unoccupied building and, consequently, no human interaction was considered. Similarly, Yin, Kiliccote, and Piette (2016) highlighted that sub-metering systems providing detailed energy consumption of each building component are generally not implemented, while the use of standards is very common to simulate the building occupancy.

However, having detailed models of subsystems is critical to develop accurate BEMs, especially if potential retrofitting measures are to be considered. Therefore, buildings need to be equipped with appropriate monitoring sensors and data acquisition systems, to collect experimental data with a high temporal resolution, typically less than

a 1 hour time resolution, over a long period of time. Notwithstanding, accurate monitoring and data acquisition systems are not often deployed in residential buildings and consequently detailed information and full experimental datasets are scarce in the literature.

In this context, the present paper contributes to this challenge by reporting the results of a comprehensive experimental campaign on a residential building located in Ireland, which was progressively retrofitted with all-electric systems and equipped with a comprehensive monitoring and data acquisition system. As described in section 2, the selected residential detached house can be considered representative of the bungalow building archetype, which represents about 40% of the overall residential stock in Ireland. The building, located in a rural area, was built in 1973 and had been progressively retrofitted with all electric equipment, including PhotoVoltaics (PV) and a Ground Source Heat Pump (GSHP) systems (section 3). The retrofit measures installed in this building are representative of specific measures which will likely be adopted by future new residential building developments.

The retrofitted all-electric house was equipped with a Home Area Network (HAN) system with more than 30 sensors for an extensive monitoring programme, thereby facilitating a comprehensive monitoring programme. The experimental data collected from the HAN system allowed the monitoring of the impact of the retrofitting measures in terms of energy consumption and carbon emissions. Moreover, the extracted dataset was used to calibrate specific building and subsystem models (section 4), facilitating the development of an accurate BEM which was then used to assess the energy saving and carbon emissions reduction potential of the retrofitted all-electric house (section 5) under different scenarios of Renewable Energy Systems (RES) penetration at a country level.

2. Irish residential sector

Generally, the building stock can be divided into residential and commercial buildings and census data or building surveys can be used to collect relevant information to characterise the building stock at country level (Mata et al., 2014). In recent years, building energy certificates and other geographical information systems have contributed to enrich existent databases and increase the data accuracy. Moreover, some European projects have compiled available information for a country or group of countries. Open data platforms (Buildings Performance Institute Europe, 2014) have started to provide open data sources for country building stocks, including Ireland. These databases have been used in the present work to provide an outlook on the Irish residential building sector.

As shown in Figure 1a, Ireland had about two million of registered houses in 2016 (Ireland Central Statistics Office (2012); Irish Central Statistics Office (2016)), most of which (about 62.8%) were built before 1996. The Irish residential building stock can be divided in four main categories: detached houses, semi-detached houses, terraced houses and apartments. The most common dwelling type is the detached house, this category being representative of about 43% of the total occupied residential buildings (Figure 1b), followed by semi-detached and terraced houses (27.8% and 16.7% respectively). Notwithstanding, the distribution of each building category is not homogeneous on a regional basis, as illustrated in Figure 2. Generally, high density population counties, such as Dublin, Cork has a greater share of apartments and semi-detached houses, while detached houses are more common in rural counties (i.e., Donegal, Mayo, etc.).

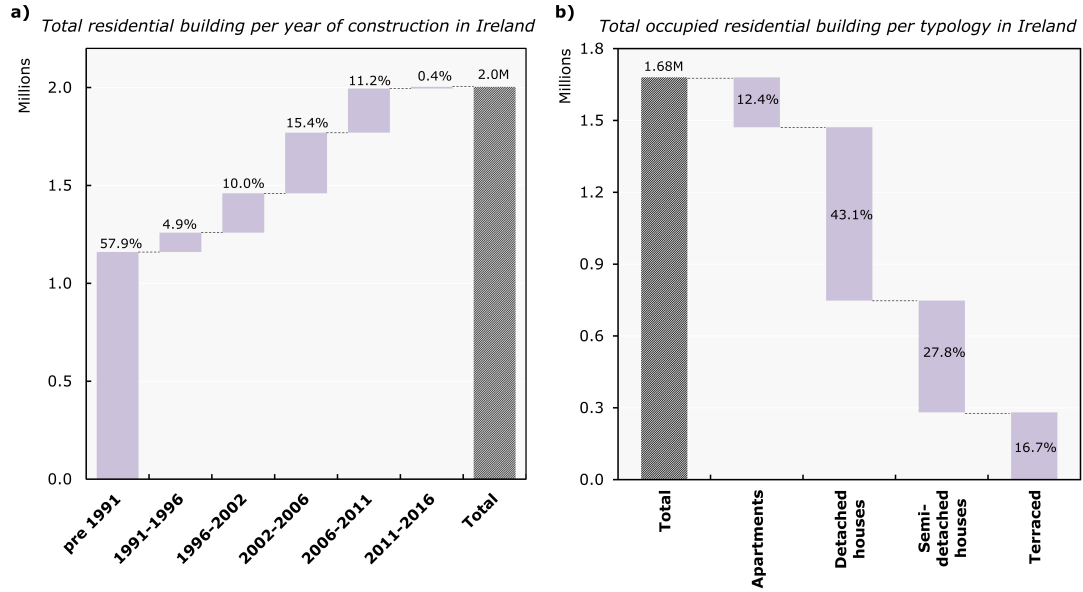


Figure 1.: a) Total residential buildings per year of construction in Ireland. (b) Total occupied residential buildings per typology in Ireland (2016). (Ireland Central Statistics Office, 2012; Irish Central Statistics Office, 2016).

According to the Irish Central Statistics Office (2016), about 40% of the total occupied domestic buildings were assessed, in order to determine their building energy ratings (BER) up until 2016. Table 1 indicates that newer buildings (2005-2016) show a relative improvement of their energy performance resulting from higher building energy standards which were progressively introduced arising from new European regulations commencing from 2007. However, most of the residential buildings fall into lower BER categories (i.e., C-G), especially the older ones, which represent the greatest share of the overall building stock (Figure 1a). Therefore, a significant energy saving potential can be achieved by introducing substantial retrofitting measures to improve the energy performance of existing residential buildings.

| Percentage of buildings per BER class in Ireland | | | | | | |
|--|-----|-----|-----|-----|-----|-----|
| Period of construction | A | B | C | D | E | F-G |
| pre 1977 | 0% | 3% | 18% | 25% | 20% | 33% |
| 1978-1999 | 0% | 5% | 39% | 36% | 13% | 7% |
| 2000-2004 | 0% | 8% | 58% | 24% | 7% | 3% |
| 2005-2009 | 1% | 35% | 50% | 10% | 3% | 1% |
| 2010-2016 | 61% | 35% | 4% | 1% | 0% | 0% |

Table 1.: Building energy ratings (BER) of residential buildings per year of construction in Ireland (Irish Central Statistics Office (2016)).

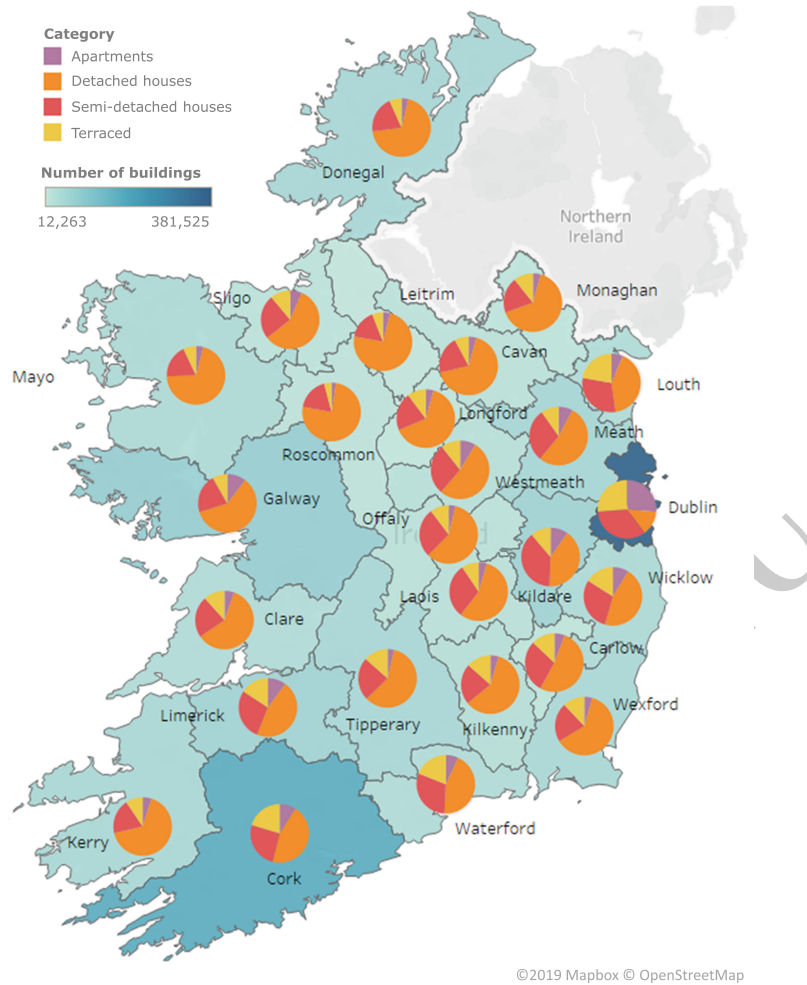


Figure 2.: Distribution of Irish building stock for each building category and county (Irish Central Statistics Office, 2016).

3. Case study

The selected building in the current work is a detached house, representative of the associated building archetype and typical of the majority of the Irish building stock and the most common single building category, as outlined in section 2. It was constructed in 1973 with a high thermal performance specification for its opaque fabric elements (equivalent to the current building standards), compared to the contemporary standards at the time of construction. In 2013, a PV system was installed and, a few months later, the combination of a GSHP for space heating and a heat recovery ventilation system replaced the existing conventional boiler. In 2014, the windows were replaced with triple glazed systems and solar thermal collectors were installed for the supply of Domestic Hot Water (DHW). Finally, an electric car replaced a conventional gasoline automobile for the household transportation needs since the summer of 2012. This electric car is charged from the dwelling electrical system.

The retrofitted building thermal performance and characteristics are similar to the average residential dwelling outlined in the 2020 scenario research published in the Res-

idential Energy Roadmap for Ireland (SEAI, 2011a). Various scenarios are described in the study, in which the reduction levels of CO_2 emissions for different retrofit measures were estimated to be between 4000 and 5000 kg of CO_2 per annum per household. The report indicates that the maximum reduction is achievable with a higher penetration of solar thermal and photovoltaic, storage heating and heat pump systems (SEAI, 2011b). As illustrated in Table 2, the majority of technologies for carbon emissions and RES integration reported in the research are present in the test bed building case study of this study.

Table 2.: Smartgrid Roadmap: Enabling technologies to facilitate RES integration and the reduction of carbon emissions (SEAI, 2011a)

| Technologies | Facilitate integration | Reduce emissions | Test Bed |
|-------------------------|------------------------|------------------|----------|
| Smart meter system | Yes | No | Present |
| DHW Electrification | Yes | No (only HP) | Present |
| Heating Electrification | Yes | Yes | Present |
| Electric vehicle | Yes | Yes | Present |
| Renewable energy | No | Yes | Present |
| Home area network | Yes | No | Present |

Some of the new systems installed in the building have also been identified by the Irish Commission for Energy Regulation as appropriate to provide energy flexibility to the grid. These technologies, if adopted in the residential sector, would enable demand response programs in the Irish power system (Single Electricity Market Committee, 2011). Their presence in the test bed building is also reported, except for the frequency response capabilities, which would typically be enabled by home automation systems. However, the rural position of the house and the associated network distribution system layout, results in the dwelling being located on the terminal side of a distribution branch. In this location, the electricity supply is more prone to voltage fluctuations that mitigate against the implementation of frequency response measures.

In the following sub-sections, a description of the main building sub-systems is presented, considering pre-retrofitted and retrofitted all-electric configurations. A picture of the building and the modelled geometry are shown in Figure 3. The house is divided in 12 zones (rooms) and an unused attic space at roof level. Two temperature sensors were installed, one in the main living area and one in the corridor, both wired to the HAN.

3.1. Thermal envelope and building physics

The test-bed house, located in eastern Ireland, is a single storey building, constructed using a two leaf concrete wall with cavity insulation. Hence, the inner walls exhibit significant passive thermal energy storage capacity. The total surface area of the exterior walls is $187 m^2$, not including windows and external doors (there are two doors with $5.4 m^2$ and $33 m^2$ window area). The roof is covered with slate and it has a surface area of $279 m^2$. The roof does not have insulation, while the ceiling is covered with tiles to ensure both acoustic and thermal insulation. On top of the tiles, a $200 mm$ layer of fibreglass ensures high thermal resistance due to its low thermal conductivity ($0.04 W/mK$). The floor area is $208 m^2$, and the overall window to wall ratio is 15%, with a 22% and 10% ratio on the south and north facades, respectively.

Although its architectural characteristics are those of a typical rural Irish bungalow

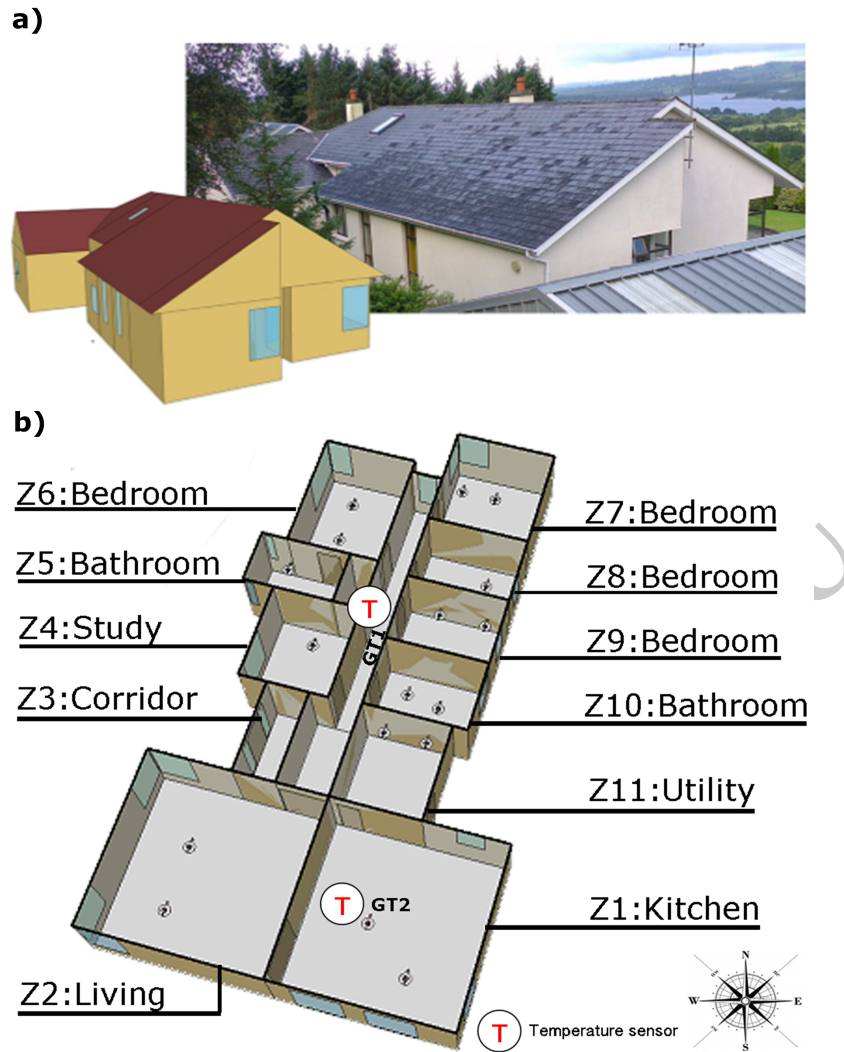


Figure 3.: a) Aerial view and EnergyPlus simulation model of the test building (Palonetto, De Rosa, et al., 2019). b) Internal sketch of the building with orientation and installed temperature sensors.

dwelling of the 1970s, its fabric specifications are very close to the current Irish building regulation values as outlined in Table 3. The difference between the pre-retrofitted and all-electric configurations in the building architecture and thermal envelope was the replacement of the aluminium double glazed windows with triple glazed windows with an air cavity of 13 *mm* and PVC frame. Moreover, an additional insulation layer was added to the ceiling to give a U-value of 0.21 W/m^2K .

3.2. HVAC systems

The heat emitters are conventional radiators located in all rooms except the bedrooms, which are heated by electric fan convectors. Additionally, a 5 kW wood fired stove is located in the kitchen, which the occupants use daily from 6 pm to 10 pm during the whole heating period. The stove affects the energy performance of the house and it

Table 3.: U Value data of different building elements for the pre-retrofitted and all-electric building models compared to the Irish building regulation standards (Irish Government, 2011)

| Building element | U-Values (W/m^2K) | | |
|------------------|-----------------------|--------------|------|
| | Pre-retrofitting | All-electric | IBRS |
| Walls | 0.21 | 0.21 | 0.21 |
| Roof | 0.25 | 0.21 | 0.16 |
| Windows | 2.6 | 1.7 | 1.6 |
| Floor | 0.21 | 0.21 | 0.21 |

has an impact on the thermal conditions of the kitchen and the adjacent living room, offsetting the heat demand of the two zones. Considering the space heating patterns of the occupants, the heating period was set from the 1st October to the 30th April. The thermostat was installed on the North-facing wall in the corridor (Z3 in Figure 3b). The building internal set point temperatures, which are measured in the hallway of the dwelling, are shown in Table 4. These were defined in accordance with the schedule and preference of the occupants.

The pre-retrofitted house model was heated with a 17 kW kerosene boiler based on a supply/return water temperature difference of 10°C. The design water outlet temperature, according to the manufacturer technical specifications, was set to 80°C. A stoichiometric report estimated the efficiency of the boiler to be 85%. The analysis of the utility bills was used to estimate the heating energy consumption of the building before the retrofit. The estimated yearly average quantity of kerosene necessary to heat the house was 943 l, that provides 9,424 kWh. Using an average price of €0.84 per litre (retrieved from historical bill data), heating the house with a conventional boiler amounted to €792 per year.

Table 4.: Thermostatic setpoints - User Preferences

| Time of day | Weekdays | Weekends |
|----------------|----------|----------|
| 00:00 to 06:30 | 19 °C | |
| 06:30 to 09:00 | 18 °C | |
| 09:00 to 16:00 | 16 °C | 20°C |
| 16:00 to 19:00 | 18 °C | |
| 19:00 to 00:00 | 18 °C | |

In the all-electric house, the space heating system is a 12 kW (thermal output) GSHP. The heat pump extracts energy from the ground using a ground loop system. Measurements indicated that the water source temperature varied over the heating season between 6-8°C over the winter period (Oct-May). For the provision of thermal energy storage, the heat pump was equipped with a hot water storage tank of 0.8 m³. The system, illustrated in Figure 4a, was installed in April 2013. The initial preference of the householder was to operate the heat pump only during the night time (between 2300 hrs to 0800 hrs), taking advantage of the low electricity tariff, and with a hot water supply temperature not higher than 50°C to achieve a higher Coefficient Of Performance (COP). Thus, between the times specified, the heat pump charges the hot water tank, while during the daytime the space heating load is covered by the hot water tank.

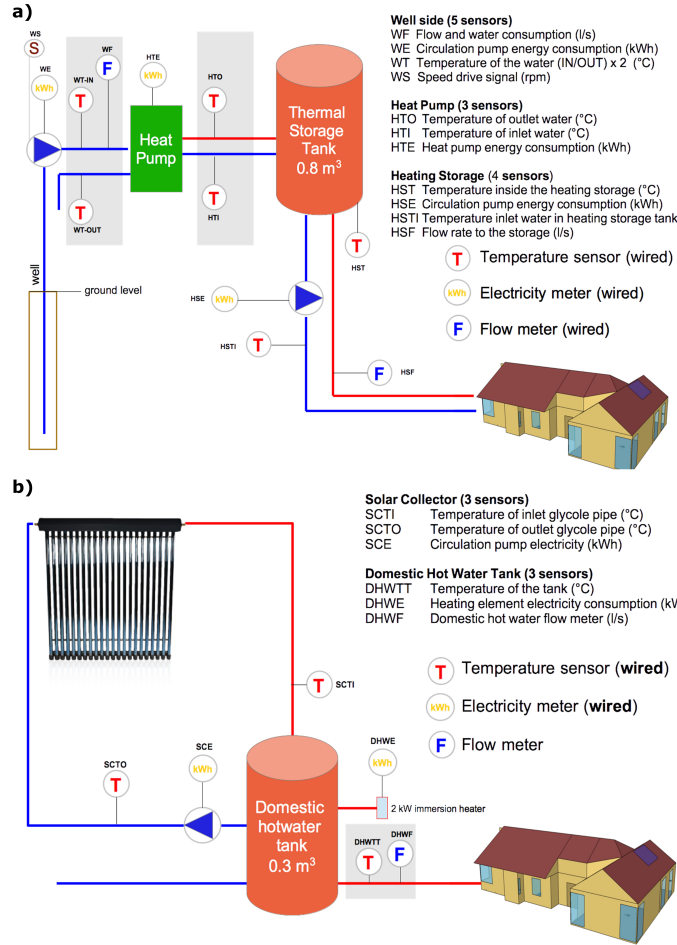


Figure 4.: Schema and sensor metering details of: a) GSHP. b) Solar DHW system.

The DHW is provided by two solar thermal collectors, each consisting of 30 vacuum pipes and feeding a 250 litre water tank. The overall surface area of the solar collectors is 6.15 m^2 . The solar collectors are placed on the roof, on a south west slope with an inclination of 35 degrees. As illustrated in Figure 4b, two stainless steel pipes connect the solar panels to a heat exchanger installed in the storage tank located in the utility room 10 meters away. An electric pump ensures the circulation of the glycol from the heat exchanger to the vacuum pipes when the temperature difference between the glycol at the solar panel (SCTI) and the storage tank temperature (DHWTT) is above $5 \text{ }^\circ\text{C}$. A 2 kW immersion resistance heater in the water tank provides auxiliary heating during winter or cloudy days. The immersion heater uses a thermostatic temperature controller or can manually be operated.

The pre-retrofitted building was naturally ventilated, facilitated by two air intake grilles which contribute to the building ventilation rate. Air ventilation and infiltration rates were taken into account by assuming an air permeability upper limit of $7 \text{ m}^3/(\text{hm}^2)$ in accordance with the Irish building regulations. In the all-electric building, a Heat Recovery Ventilation (HRV) system was installed with an average sensible heat transfer effectiveness of 80%, which operates only during the heating period with a specific fan power of 60 W and volume rate of 0.7 W/l/s . The air permeability upper limit is assumed to have been reduced by 28% to $5 \text{ m}^3/(\text{hm}^2)$, because of the

additional sealing works on walls, ceilings, window frames and floor skirtings. The air permeability coefficient utilised refers to new building construction as reported in the Energy Trust practical guide (EnergyTrust, 2005) and in Sinnott and Dyer (2012). These values have been used because it was not possible to perform a building blower door test.

3.3. PV system and electric car

The array of the installed photovoltaic panels has a nominal power of 6 kW_p and it is located 30 meters from the dwelling, facing South with an inclination of 30 degrees. Thirty PV panels, each with a nominal power of 200 W_p, were positioned in three rows of 10 panels each. The inverter installed was a single-phase and its efficiency is 95% as per the manufacturer technical specifications. Each PV panel is composed of 126 poly-crystalline silicon solar cells. The output tolerance of each panel was to within 0/+5 W. The total inclined surface of the PV system was 51.9 m² while the occupied surface area was 70 m². Figure 5 illustrates the electricity meter (PVE) used to measure the PV production. The meter is located between the inverter and the bi-directional general meter between the house and the power grid.

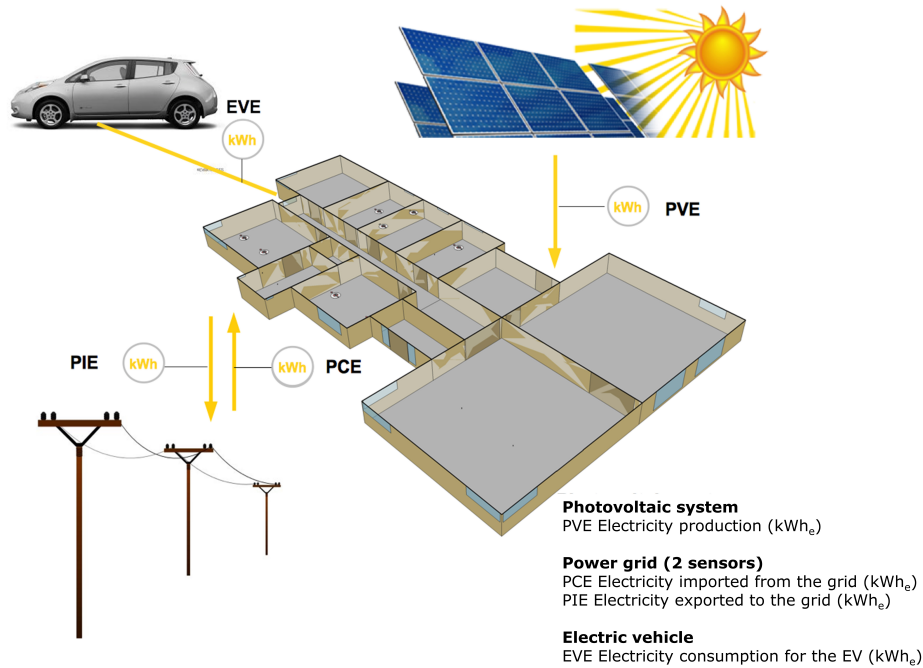


Figure 5.: Photovoltaic system, electric vehicle and associated sensors.

A Nissan Leaf (2011 model) with a 24 kWh battery pack is used for the daily commute of the building owner of approximately 50 km, which is equivalent to half of its autonomy range. According to the manufacturer data (Masoum, Deilami, Moses, & Abu-Siada, 2010), the maximum charging power rate is 3.3 kW. The car is charged each night, and, during winter the heating element in the car is activated during commuting. The connection to the electricity system, as illustrated in Figure 5, and it has a stand alone meter.

3.4. HAN system

Forty-three sensors were installed in the house during the experimental phase. The sensors were linked to the HAN through two gateway devices connected via an IEEE 802.03 infrastructure (Keiser, 1989). The installed HAN router enabled a home wireless network based on standard IEEE 802.11 and provided wired connection for four Ethernet ports. The device was mounted in the attic zone and provided network coverage and internet access for the majority of the building. In the attic zone, a wired gateway managed 31 sensors. These were linked to the gateway through five MODBUS lines (Modbus, 2004).

Five MODBUS lines were utilised and these are described in Table 5. For each subsystem, the MODBUS line is indicated and the sensors are organised into four different categories: temperature, flow, energy and other. In the latter category, beside the two humidity sensors connected to the HRV for the air extraction and supply, the ground loop inlet circulation pump speed was recorded using a pulse open contact signal. A wireless ZigBee network was installed in the building with an additional twelve electricity and temperature sensors. After the installation of the ZigBee network, frequent disconnections of the sensors occurred, and a degradation of the WiFi network transmission rate and reliability was noted. As confirmed by Yi, Iwayemi, and Zhou (2010), IEEE 802.11 and ZigBee coexistence can cause interference which can compromise the data acquisition.

4. Numerical model

4.1. Thermal envelope and HVAC

An EnergyPlus model was developed with 15 different thermal zones, one for each room and three for the attic space. The complex shape of the roof required the attic space to be divided into three different zones. The U-value estimation of the building envelope utilised up to 13 different composite construction materials for certain elements. The components were modelled after several inspections of the house and a survey conducted with the owner. All the construction elements use generic building materials, except for the walls and floor, which were retrofitted in 2011 with a new insulation layer before the current research began.

The air exchange with the external environment was modelled for the pre-retrofitted and all-electric building Building Energy Simulation (BES) model separating the ventilation and the infiltration. On the pre-retrofitted model, following the trends of buildings with similar construction features, the ventilation rate was adjusted to an annual average value of close to 1 Air Changes per Hour (ACH) with the exception of the kitchen and bathroom, where the respective values were 1.5 ACH (Dimitroulopoulou, 2012). In the all-electric model, ventilation was achieved exclusively by the operation of the HRV, whereas in summer by natural ventilation (window opening). During the heating period, for ventilation purposes, the building is divided into two sections with the following ACH settings: a kitchen/living/bathroom zone (ACH 1.5) considering the cross air mix between the zones and a sleeping/utility zone (ACH 1.0). Proportional infiltration flow rates are dynamically calculated at each simulation time step based on the indoor and outdoor conditions, i.e., temperature, wind speed and direction (EnergyPlus Engineering Reference, 2015).

Table 5.: Test-bed house, installed sensors and reference index

| System | Line | Figure | Temperature [°C] | Flow rate [l/s] | Energy [kWh] | Other [W,%RH] |
|------------------|-------------|---------------|-------------------------|--|------------------------------|-----------------------------|
| Thermal Envelope | I | 3b | Corridor (GT1) | - | - | - |
| | | | Living area (GT2) | - | - | - |
| | | | Outdoor air (GT3) | - | - | - |
| Heat Pump | II | 4a | Well inlet (WT-IN) | Well inlet (WF) | Well inlet pump (WE) | Pump speed (WS) |
| | | | Well outlet (WT-OUT) | | HP consumption (HTE) | |
| | | | Water inlet (HTO) | | | |
| | | | Water outlet (HTI) | | | |
| TES | II | 4a | TES outlet (HST) | TES outlet (HSF) | TES inlet pump (HSE) | - |
| | | | TES inlet (HSTI) | | | |
| DHW | III | 4b | Solar inlet (SCTI) | Tank | Heating element (DHWE) | - |
| | | | Solar outlet (SCTO) | | Solar circulation pump (SCE) | |
| | | | Tank | | | |
| EV | IV | 5 | | | Consumption (EVE) | |
| PV | IV | 5 | | | Solar generation (PVE) | |
| Other | IV | 5 | | | Grid immission (PIE) | |
| | | | | | Grid consumption (PCE) | |
| HRV | V | - | Extraction air (HTINS) | | Fan (HEF) | Humidity extraction (HHINS) |
| | | | Immission air (HTS) | | | Humidity immission (HHS) |
| | | | Exhaust air (HOUT) | | | |

4.2. HVAC and DHW systems

The heating system (GSHP) was modeled in EnergyPlus using a parameter estimation or an equation-fit model (EnergyPlus Engineering Reference, 2015). The parameter estimation model technique solves the objective function using an unconstrained optimisation algorithm. The methodology converges to an estimate of the model parameters. It is mostly used for the extrapolation of the model from measured data when the unit specifications are partial or in certain cases, absent. According to Ellis, Torcellini, and Crawley (2008), the parameter estimation model can be more accurate than the equation fit, however it is computationally more intensive and the technique does not guarantee the convergence of the calculation at each time step. The equation fit model uses four equations to predict the behaviour of the heat pump execution cycle. It is mostly used when the equipment specification is available. In the present work, the equation fit was preferred as a better and more consistent technique to model the system, since heat pump data was available. The input variables for using the equation fit technique and a reference to the installed sensors as summarised in Table 5, are as follows:

- Load side inlet water temperature (HTI);
- Load side outlet water temperature (HTO);
- Source side inlet temperature (WT-IN);
- Source side water flow rate (WF);

Regarding the DHW system, it was assumed that the glycol fluid has a concentration of 30%, which is based on best practise (Kalogirou, 2004). Because of the presence of only one sensor in the middle of the water tank (DHWTT), as shown in Figure 4b, the tank was modelled as fully mixed. Consequently, any thermal stratification in the water tank was not taken into account. The solar system installed is an evacuated tubes panel. According to EnergyPlus Engineering Reference (2015), EnergyPlus uses a generic model equation labelled as *FlatPlate* which adheres to the ASHRAE standards (ASHRAE, 2002) and can also be used to model evacuated tube systems. The thermal and optical performance parameters of the system were obtained from the technical specification sheets of the manufacturer.

4.3. PV system and electric car models

Each PV panel was modelled using a single diode equivalent circuit (EnergyPlus Engineering Reference, 2015). In this model, the delivered current is directly dependent on the solar radiation at the surface and on its temperature. The EnergyPlus input module has an angle modifier to infer how the reflectivity of the module varies with the angle of incidence. The output of the module simulation includes an open-circuit voltage, short-circuit current and maximum power point voltage and current. The inverter efficiency was set at 0.95 according to the technical spreadsheet of the manufacturer. The 30 meters distance between the inverter and the DC cables was considered relevant in terms of cable losses and this was modelled accordingly in EnergyPlus.

According to Smith (2010), the energy consumption by electric vehicles depends on the season due to the air conditioning requirements of the cabin, which can significantly affect the energy performance of the car. The electricity consumption of the modelled electric vehicle (EV) was assumed of 150 Wh/km in summer and 250 Wh/km in winter. The assumptions were based on the work of Marra et al. (2012) and confirmed by the estimate calculated by Next Green Car (NextGreenCar, 2016). Moreover, it

is noted that 2011 Nissan Leaf versions have a ceramic Positive Thermal Coefficient of resistance (PTC) heating element with peak energy consumption of 5 kW (Shin, Sim, & Kim, 2016). However, in the EnergyPlus model, the operation of the heating element was embedded in the winter average consumption per kilometre, assuming the energy to heat the car was supplied by the EV battery.

4.4. Internal gains and occupancy profiles

Two adults occupy the house and the associated heat gains were determined and spatially mapped within the building model. Domestic hot water usage patterns, the use of electric equipment and lighting, and the respective distribution of internal heat gains were calculated based on the national time of use survey resident activity data and, then, adjusted to match the electricity profile (Commission for Energy Regulation, 2011). For privacy reasons, the activity patterns of the occupants were not tracked using the installed sensors. However, a bottom-up approach, based on time of use activity data was used for generating, at an individual room level, occupancy profiles and disaggregated electrical appliance loads and lighting load profiles at a 15 minute time resolution (Neu, Oxizidis, Flynn, Pallonetto, & Finn, 2013).

The 2005 survey data utilised included 567 households and reported the user activity at a fifteen-minute time resolution for weekdays and weekend days (McGinnity, Russel, Williams, & Blackwell, 2005). Each participant recorded the activity undertaken, at home or away from home, for each time-step by choosing the most appropriate activity code from a list of 26 keys. The data was used to build a Markov Chain Monte Carlo model for each activity reported in the survey. In the current work, the developed activity model was embedded and adapted for the EnergyPlus test bed building model. Therefore, daily power consumption patterns, for the household size and the different day types, were quantitatively and qualitatively adjusted against metered electricity data and occupant survey data. The synthesised profiles were calibrated with the appropriate occupant feedback to replicate better the real-life activity patterns.

4.5. Calibration procedure

A building simulation model produces an energy demand or generation profile for each system modelled. When the simulation output and the metered data do not match, the modeller can modify the input parameters to reduce the error. This iterative process is called calibration and it is aimed at improving the accuracy of numerical models. There are five main categories of calibration methodologies: manual, iterative, graphical, statistical and automated (Raftery, 2011). The utilisation of one or more methodologies depends mainly on the purpose of the model, building system complexity, data availability and resolution (Coakley, Raftery, & Keane, 2014). Moreover, various data sources supply different levels of insight of the construction and can contribute to the calibration process (Royapoor & Roskilly, 2015). Typical data providers for a calibration process are: (A) direct interview with building stakeholders, (B) data sensor logging, (C) technical documentation, (D) project plans, (E) benchmark case studies, (F) spot or short-time measurements, and (G) policy and regulation.

In the current research, the calibration process was divided into two main stages. The pre-retrofitted building was calibrated using direct interviews with manufacturer companies (A), surveys with the building owner (A) and spot measurements (F). During the first phase, there were no high-resolution sensors in place. Consequently, the

calibration of the pre-retrofitted model was partial and relied on the utility electricity meter and kerosene bills. The thermal performance of the model was also integrated and compared with current regulations (G). In the all-electric model, the building geometry description was extracted from the pre-retrofitted model. The 3D geometry was expanded with new systems using technical documentation (C), which were utilised to complete the equation parameters of each system. Moreover, the model was further tuned with the available sensor data (B).

The calibrated model was used to decompose the thermal and electricity consumption pattern for each sub-system, to support recommendations and retrofit measures, to schedule changes or control settings and overall to test the control algorithms developed in the EMS. The process was divided into four main steps as described in Mustafaraj, Marini, Costa, and Keane (2014):

- Collect, classify and clean available data;
- Modify the BES model subsystem equation parameters based on the documentation and sensor data;
- Compute the established statistical indexes to assess the calibration accuracy by comparing the predicted output with the measured data;
- Reiterate from step 2, if the calibration acceptance criteria are not met.

ASHRAE acceptance criteria were used to calibrate the all-electric model with 2014 measured data from the site which consists of a dataset with a 15 minute time resolution (Mustafaraj et al., 2014). Given that the overall objective was to calibrate the building demand flexibility as secondary reserve and not for frequency response, a 15 minute resolution was considered to be sufficient. This can be justified in the context of the technical specifications associated with the provision of ancillary services in the Irish electricity market (Commission for Energy Regulation, 2013). Two statistical indexes were selected to assess the accuracy of the calibrated model, the Mean Bias Error (MBE) and Cumulative Variation Root Mean Squared Error (CVRMSE) calculated as shown in Eq. 1 and Eq. 2 respectively, where the term m_i and s_i represent the measured and simulated output, while N is the number of data points in the interval and \bar{m} is the average of the measured data points.

$$MBE(\%) = \frac{\sum_{i=1}^N (m_i - s_i)}{\sum_{i=1}^N m_i} \quad (1)$$

$$CVRMSE(\%) = \frac{\sqrt{(\sum_{i=1}^N \frac{(m_i - s_i)^2}{n})}}{\bar{m}} \quad (2)$$

Although MBE suffers from a cancellation effect, the use of two different indexes can provide a balanced assessment. Furthermore, these two indexes are the most common in the building modelling literature (Raftery, 2011; Reddy, Maor, & Panjapornpon, 2007; Westphal & Lamberts, 2005) and are recommended by ASHRAE as standard indexes for building calibration. In particular, ASHRAE (2002) establishes a 5% limit for MBE and a CVRMSE 15% threshold for calibration using monthly data. Using hourly data points, the suggested limits are 10% and 30% for MBE and CVRMSE, respectively. There are no standard calibration thresholds for higher resolution than an hourly basis (Coakley et al., 2014).

5. Results

5.1. Model calibration

The building did not have a monitoring and data acquisition prior to retrofitting. Therefore, the EnergyPlus model of the pre-retrofitted building was calibrated using historical electricity and heat demand data. The only available data to estimate the heat demand was historical heating fuel consumption records and the thermostatic setpoints, as confirmed by the building owner. An experimental on-site stoichiometry test revealed a boiler efficiency of 85%. The total yearly average amount of kerosene required to heat the building was 1,886 litres that provides approximately 19,200 kWh (conversion factor of 10.18 kWh/l). Finally, historical electricity bills were used to determine an average annual electricity consumption, which were equal to 2800 kWh/year. The Energy Plus model of the pre-retrofitted building was then calibrated on this basis achieving results within the ASHRAE monthly calibration standards.

The retrofitted building EnergyPlus model shown in section 4 was calibrated by using the data collected over the year 2014. A total of 8760 hours and approximately 35000 data points for each of the sensors were collected during the experimental campaign. The following sections describe the procedure and results obtained by the calibration of each subsystem considered.

5.1.1. Thermal envelope and HVAC system

As described in section 4.4, the building was occupied by two adults for the whole duration of the research. Since the activity patterns were not tracked for privacy reasons, it was not possible to calibrate the model over the whole season according to the ASHRAE criteria. Moreover, given the limited floor area of the building, the manual operation of appliances and windows affected the hourly based calibration, despite the accuracy of the building elements and systems modelled. These issues are common in the calibration process for small buildings, when the end user activities are not tracked and they affect the internal heat gains and, consequently, the accuracy of the calibration (Hopfe & Hensen, 2011). For these reasons, the calibration was carried out using metering equipment for a short time period (Short-Term Energy Monitor test (STEM)) when the building was not occupied (Coakley, 2014).

The calibration of the thermal envelope was performed on five selected days when the occupants were not in the building. The calibration results for the five days are illustrated in Table 6. During these five days, the measured temperature decay of the building versus the model was used to calibrate the thermal envelope. It can be noted that both the MBE and the CVRMSE are below the hourly ASHRAE standards (ASHRAE, 2002). Similarly, Figure 6 illustrates the temperature decay of the simulation versus the sensor data for the 1st of May. The MBE index on the secondary axis of the figure is based on a 15 minute resolution. The internal temperature of the simulation minus the measured data at 01:00 hrs shows a $0.5^{\circ}C$ difference while at 23:30 hrs the difference is observed to be $-0.3^{\circ}C$. Since the weather file shows a negative bias for solar radiation, it resulted in a constant internal temperature drop in the simulation, while the measured internal building temperature increases due to the solar heat gains during the day. However, from the calibration perspective, the difference was estimated within $\pm 0.5\%$ MBE and is therefore considered negligible.

Figure 7a shows the results obtained from the calibration of the GSHP carried out with the experimental data collected during the whole of 2014. It is noted that the

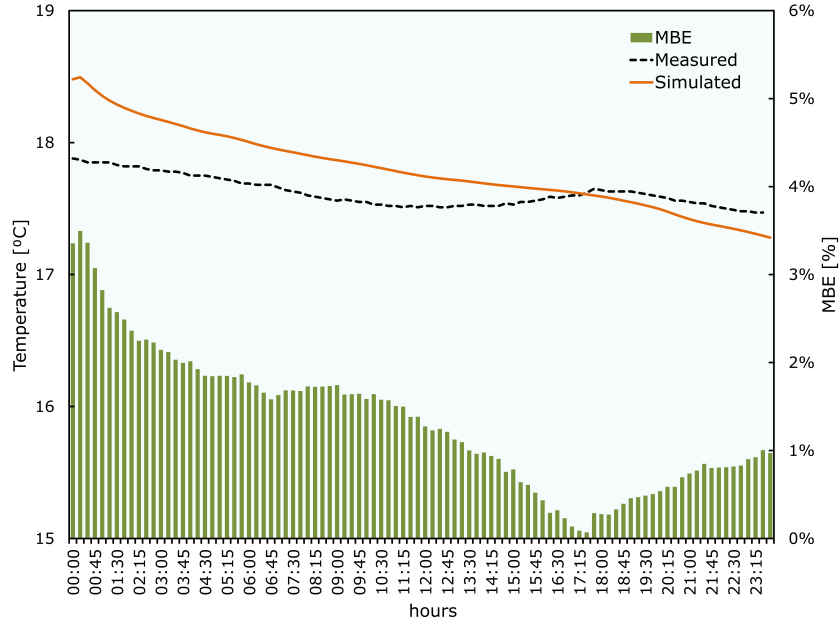


Figure 6.: Thermal envelope calibration for a selected day (1st May 2014).

Table 6.: Thermal envelope calibration for selected days (15-min resolution)

| Selected day | MBE min% | MBE avg% | MBE max% | CVRMSE avg% |
|-----------------|----------|----------|----------|-------------|
| 17 March 2014 | -1.1 | 4.13 | 9.5 | 4.46 |
| 30 April 2014 | 1.4 | 3.62 | 4.8 | 3.51 |
| 01 May 2014 | -0.9 | 1.01 | 3.4 | 1.19 |
| 13 October 2014 | 0.6 | 4.06 | 11.2 | 3.25 |
| 16 October 2014 | 5.1 | 9.21 | 16.9 | 3.96 |

associated calibration was within ASHRAE thresholds (ASHRAE, 2002). Specifically, the monthly calibration resulted in a CVRMSE of 3.78% and a MBE of -0.61%. Two CVRMSE peaks (November and February), caused by a difference between the operation scheduled for the wood-burning stove in the model and the retrieved data, can be also observed. Furthermore, Figure 7b shows the cumulative annual electricity consumption of the GSHP with a 15 minute timestep resolution during the GSHP operations. As illustrated in the figure, the occupants decided to sporadically switch ON/OFF the heat pump, thereby bypassing the tank storage to adjust the inside temperature during the period between the 15/04 to the 31/05. The unconventional operation of the GSHP is evident in the graph, and it has skewed the 15-minute calibration of the whole heating season which results in an MBE of 2% and a CVRMSE of 14.7%.

The HRV system was calibrated only on a test day where both the heat pump and the wood-burning stove were not in use. The calibration involved the tuning of two variables: the extracted air temperature (**HTINS**) and the supply air temperature (**HTS**). The external temperature was isolated from the selected weather station, while the rest of the data were retrieved from sensors installed on the heat exchanger. The schedule of the HRV in EnergyPlus was set to operate between 1000 hrs to 2100 hrs. As illustrated in the figure, besides the operational hours (1000 hrs to 2100 hrs),

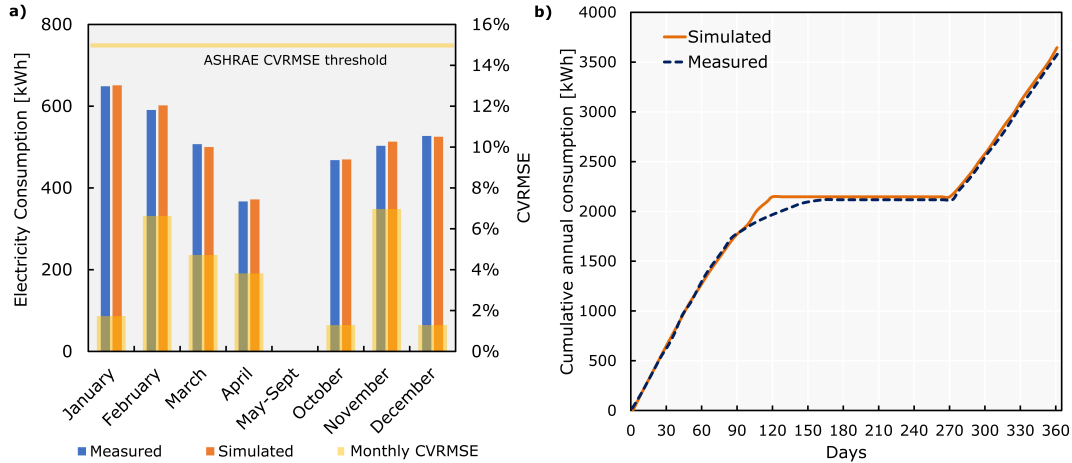


Figure 7.: a) Monthly GSHP electricity consumption. b) Annual cumulative GSHP electricity consumption.

EnergyPlus outputs a default temperature value for the supply air (**HTS**), reducing the air flow to 0 l/s. The hourly calibration resulted in a 9.7% MBE and 33.5% CVRMSE. The manual operation of the HRV and the required insulation works on the duct pipes allowed a partial calibration of the system.

Finally, the calibration process was performed on the water tank temperature utilising the data acquired by the sensor with a time resolution of 15 minutes. The heating element was switched on by the owner as domestic hot water was required. The manual operation of the 2 kW heating element represented a challenge for the calibration process. Consequently, the month of July 2014 was selected because the heating element was not used due to a significant solar irradiation. The temperature difference between the model and the simulation reached a peak MBE of 45% on the 27th of July. The hourly calibration, for the month of July, resulted in an average MBE of 17.3 % and CVRMSE of 32.5%, consequently the calibration was not possible with reference to ASHRAE criteria (ASHRAE, 2002).

5.1.2. PV system and electric vehicle

The PV model was calibrated by using 15-minute resolution data for the 12 months of 2014. Unscheduled maintenance caused the main output difference in May and during the months with less electricity generation (Nov-Dec), as well as grid disconnection caused by frequency instability, giving rise to a 5% maximum divergence. The calibration was performed for 2014 and met the hourly ASHRAE criteria. As illustrated in Figure 8a, a good match between experimental and numerical results were obtained, with average annual MBE and CVRMSE of 3.6% and 12.5%, respectively.

Regarding the electric car, it was charged overnight when electricity prices were lower. The estimated daily energy requirement of the car was 12.5 kWh in the winter and 7.5 kWh in the summer (Marra et al., 2012). During the night time charging period, the electricity drawn was assumed to follow the pattern assessed by the manufacturer (INES, 2013) and confirmed by the measured data as shown in Figure 8b. The weekday EV energy consumption was calibrated on the basis of 15-minute resolution. The calibrated model was aligned to the monitored data with an annual MBE of +/- 3.5% and CVRMSE of 10.4%.

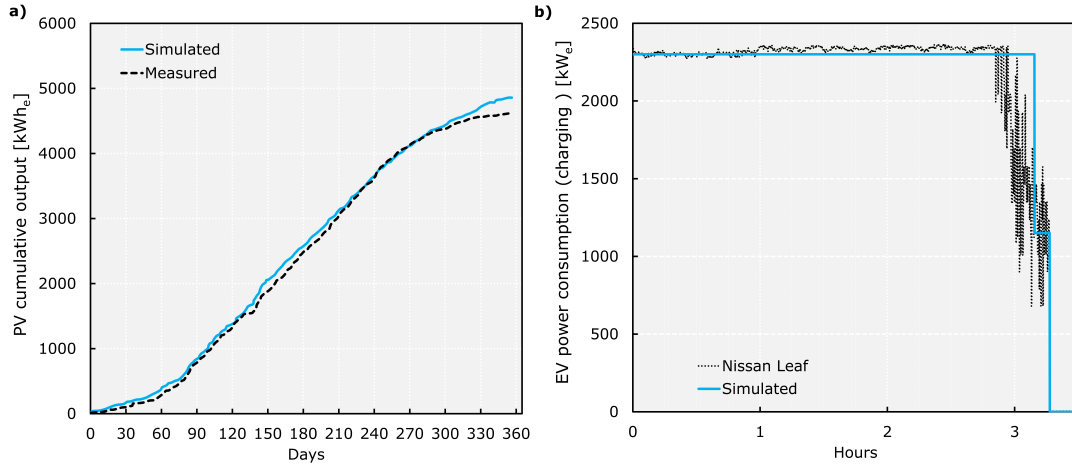


Figure 8.: a) Cumulative PV electricity generation. b) EnergyPlus charging model for the electric vehicle.

5.1.3. Overall calibration

The main challenge faced during the calibration of the building simulation model which affected the overall model accuracy, were: (i) the calibration of the manually operated systems, such as the HRV and DHW; (ii) estimation of the impact of the wood-burning stove on the internal temperature; (iii) unscheduled road trips with the EV, and other untracked activities. However, the thermal envelope, the GSHP and the PV were calibrated using data with a 15 minute resolution, resulting in compliance with the hourly ASHRAE standards. The present section, reports the results obtained in terms of overall electricity consumption of the analysed building.

Figure 9a shows the hourly based cumulative metered electricity consumption versus the simulated profile for the year 2014. Additionally, on the right vertical axis the average MBE index of the calibration for each hour is given. The graph shows divergence at 02:00 and 08:00 during the EV charging time, mainly caused by the unrecorded occupant behaviour. Moreover, the use of the wood-burning stove during the winter weekends is not captured by the occupant activity model, resulting in a heating consumption bias between 1000 hrs and 1800 hrs. The last notable difference is that some unscheduled activity at 23:00 that caused an average hourly MBE of 25%. However, the overall annual electricity consumption calibration model results having an MBE of -1.6% and a CVRMSE of 10.5%. A higher resolution for the overall electricity demand calibration was not possible since the occupant activities and, consequently, the use of appliances and domestic machinery were not tracked.

Figure 9b shows the electricity profile MBE calculated values between metered data and BES model prediction for the whole year (35,040 data points) as a frequency histogram. About 47% of the recorded absolute MBE values are below 30%, while highest frequency was recorded for absolute MBE values between 0 and 10%. Additionally, the occupant activities not captured by the model, which corresponds to an error between 91-100% in figure 9b, resulted to be equal to about 12% of the total time steps analysed.

5.2. Analysis on energy consumption and carbon emissions

On the basis of the model calibration described in section 5.1, the resulting model was used to investigate effect of the energy efficiency measures and associated carbon emissions. The analysis also takes into account an annual commuting distance of 12,000 km by the dwelling occupants. This is in accordance with the average values in Ireland (SEAI, 2017).

The results show an improvement in the overall building energy performance of the retrofitted building (i.e., all-electric scenario) compared to the pre-retrofitted one. Figure 10a shows that an annual reduction of end-use energy consumption of up to 45% can be achieved by the all-electric building. More specifically, observing the energy savings breakdown associated with the different energy systems, a saving of 63% was calculated for the case of the EV and the gasoline car, while a saving of 40% derived from the heating system accounting for the energy consumed by the boiler for space heating.

Moreover, data from the Irish electricity system operator (Eirgrid) was used to calculate the carbon footprint of the building. This data contains the Irish power grid fuel mix and the wind generation at 15-minute resolution. The average emission intensity per MWh_e from the Irish electricity system was extracted on an hourly basis for the year 2014. The Transmission System Operators (TSO) data was processed by interpolating the CO_2 emissions on an hourly basis to each associated 15-minute time step (Eirgrid, 2015). CO_2 emissions due to the kerosene boiler were calculated by using a value of $257 gCO_2/kWh_e$ (SEAI, 2012). The calibrated model was then used to assess carbon emissions patterns and environmental impact of the all-electric versus the pre-retrofitted model. Figure 10b shows the resulting annual CO_2 emissions for the pre-retrofit and post-retrofit building. The results show that the building carbon footprint of the pre-retrofit house was approximately 9030 kg of CO_2 ($43.3 kg/m^2/CO_2$) in 2014.

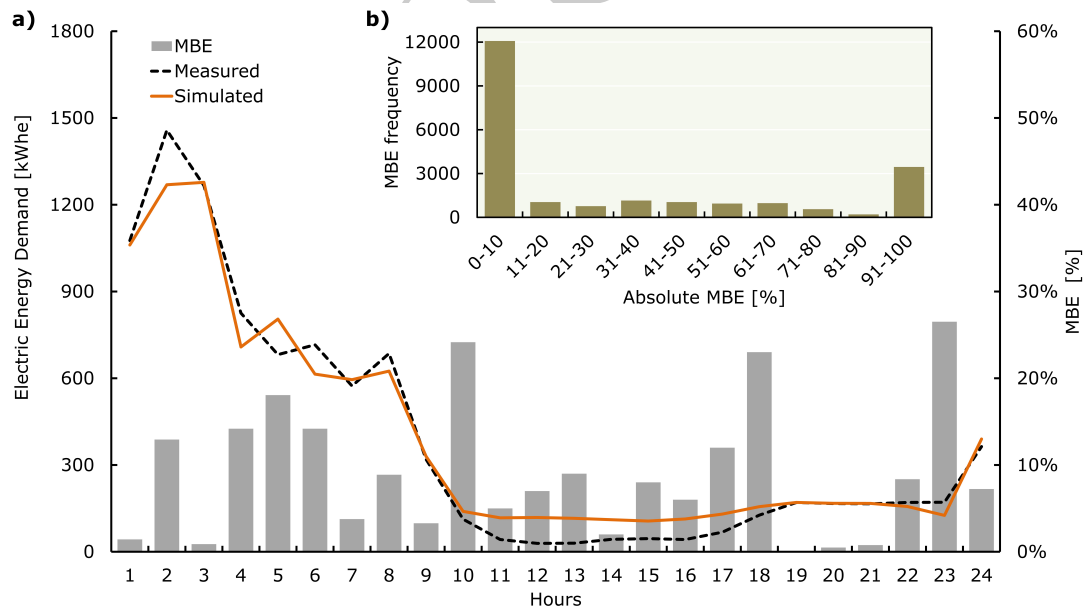


Figure 9.: a) Cumulative annual dwelling electricity consumption depicted on an hourly basis. b) Frequency histogram of the absolute MBE values for dwelling total electricity consumption.

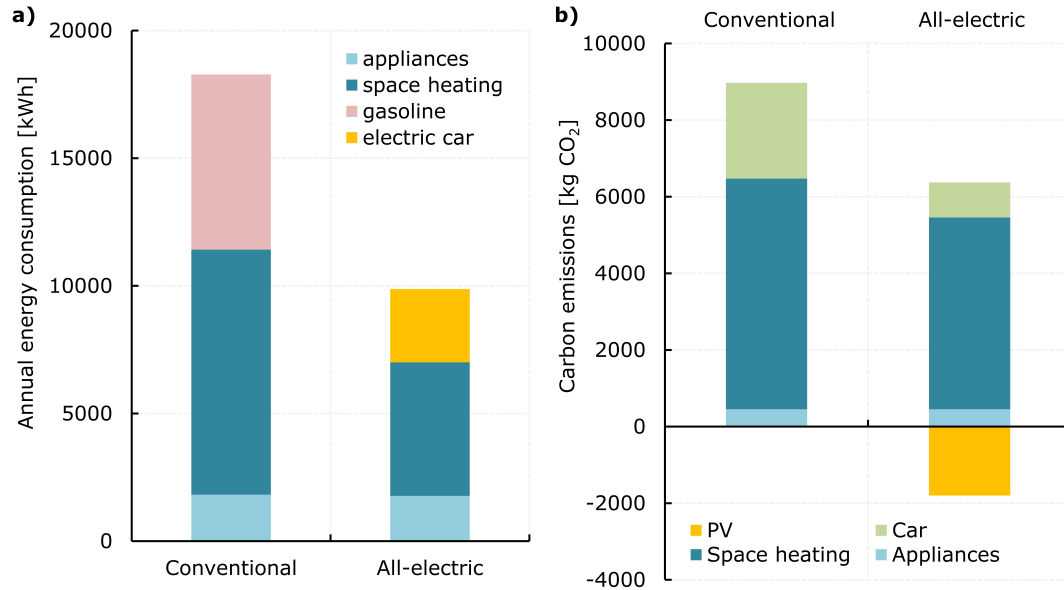


Figure 10.: Annual performance of pre-retrofitted and all-electric dwelling: (a) end-use energy consumption and (b) associated total carbon emissions.

On the contrary, the all-electric house emitted 6400 kg of CO_2 ($30.8 \text{ kg}/m^2/CO_2$), thus demonstrating an emissions reduction of approximately 28.9%. Generally, the all-electric building has a carbon emissions value 48% below building national average for 2011 (SEAI, 2013).

In order to investigate the influence of different renewable energy penetration levels, two representative days with different wind generation shares - calculated by dividing the Irish electricity demand by the the daily wind generation - were selected. These days have a similar average ambient temperature ($2.5 \text{ }^\circ\text{C}$), but differ in term of generation wind share, i.e., 20% and 4% for the high and low wind penetration scenarios, respectively. The results are shown in Figure 11 in terms of total daily carbon emissions for each scenario considered. It can be seen that the retrofitted all-electric building displays a reduction of the carbon emissions compared to the pre-retrofitted building, ranging from 4% reduction for the low wind penetration day, to 18% for the high wind penetration day.

Therefore, switching to a retrofitted all-electric building configuration may allow significant carbon emissions savings, generally depending on the penetration of RES achievable at the generation level. If a high share of RES occurs, while the emissions associated with domestic appliances remain almost the same, about 12% and 44% savings can be achieved in terms of space heating and car fuel consumption (gasoline versus electricity). However, when a low RES share occurs, carbon emission savings decrease to 4% only, mainly due to the greater emissions associated with the heating system (about 5%).

From an Irish perspective, reductions in carbon emissions could be achieved by retrofitting of selected residential building stock with all-electric technologies, when considered in conjunction with RES penetration in Ireland. As discussed in section 2, almost 60% of Irish building stock exhibit poor energy standards, falling into the lower BER categories (i.e, C-G). However, as the distribution of the building archetypes is not homogeneous, understanding the potential impact of retrofitting the residential

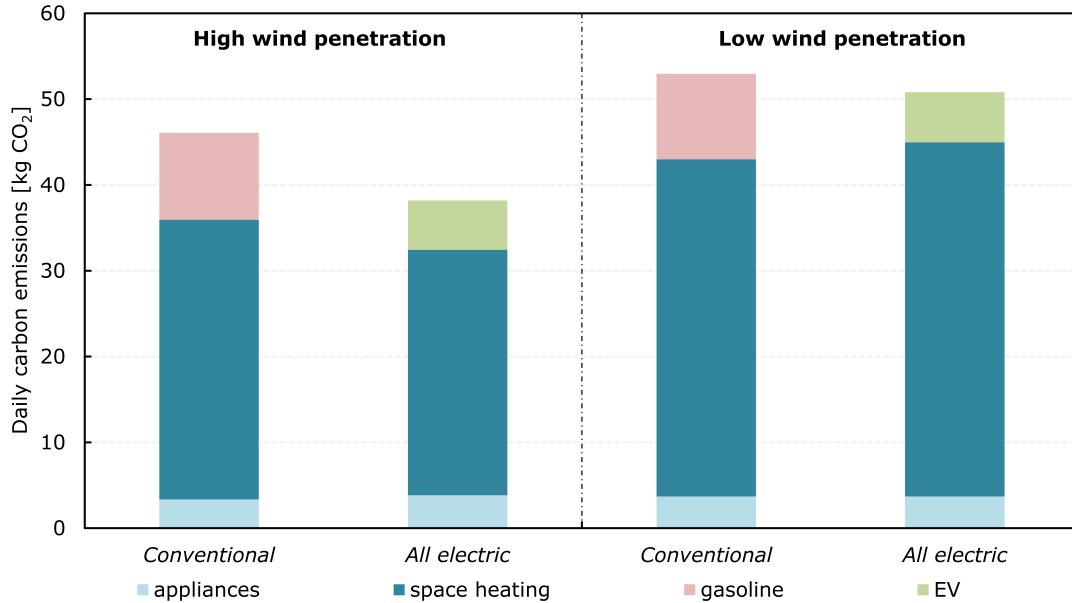


Figure 11.: Daily carbon emission from the pre-retrofitted and retrofitted (all-electric) dwelling for two representative days with high-wind and low-wind penetration.

building stock at a local regional or county level is potentially of interest. Figure 12 illustrates the potential of carbon emissions reduction for different retrofit percentages (i.e., penetration of retrofitting measures in a sub-section of building stock consisting of detached dwellings only). The baseline case is represented by a pre-retrofitted detached dwelling equipped with a boiler. The sensitivity analysis, based on two RES penetration scenarios (i.e., high wind and low wind), highlights potential carbon emissions reduction for this section of the residential sector of up to 14%. This reduction is can be associated with the building distribution and the overall population density at a county level. Therefore, in rural counties such as Donegal or Leitrim, the potential impact of a deep retrofit of detached houses is greater, whereas in urban areas such as Dublin and Cork, with less detached houses, the relative impact is lower. This is a potentially useful perspective for the evaluation of targeted policies fostering more widespread retrofitting intervention for residential detached buildings, which together with concerted deployment of smart grid infrastructure and RES to smooth grid instability and congestion, could potentially increase the overall efficiency of the building stock.

6. Conclusions

The electrification of thermal loads and transport, together with higher penetration of renewable energies at a building level, has been recognised as one possible contributor to reducing the carbon emission. Using a calibrated building model, the present paper investigated the potential energy savings associated with the implementation of retrofitting measures on an Irish residential dwelling.

A residential detached house, representative of a building archetype, which is typical of about 40% of the overall residential stock in Ireland, was selected as an experimental test bed. The building, located in a rural area, was progressively retrofitted with

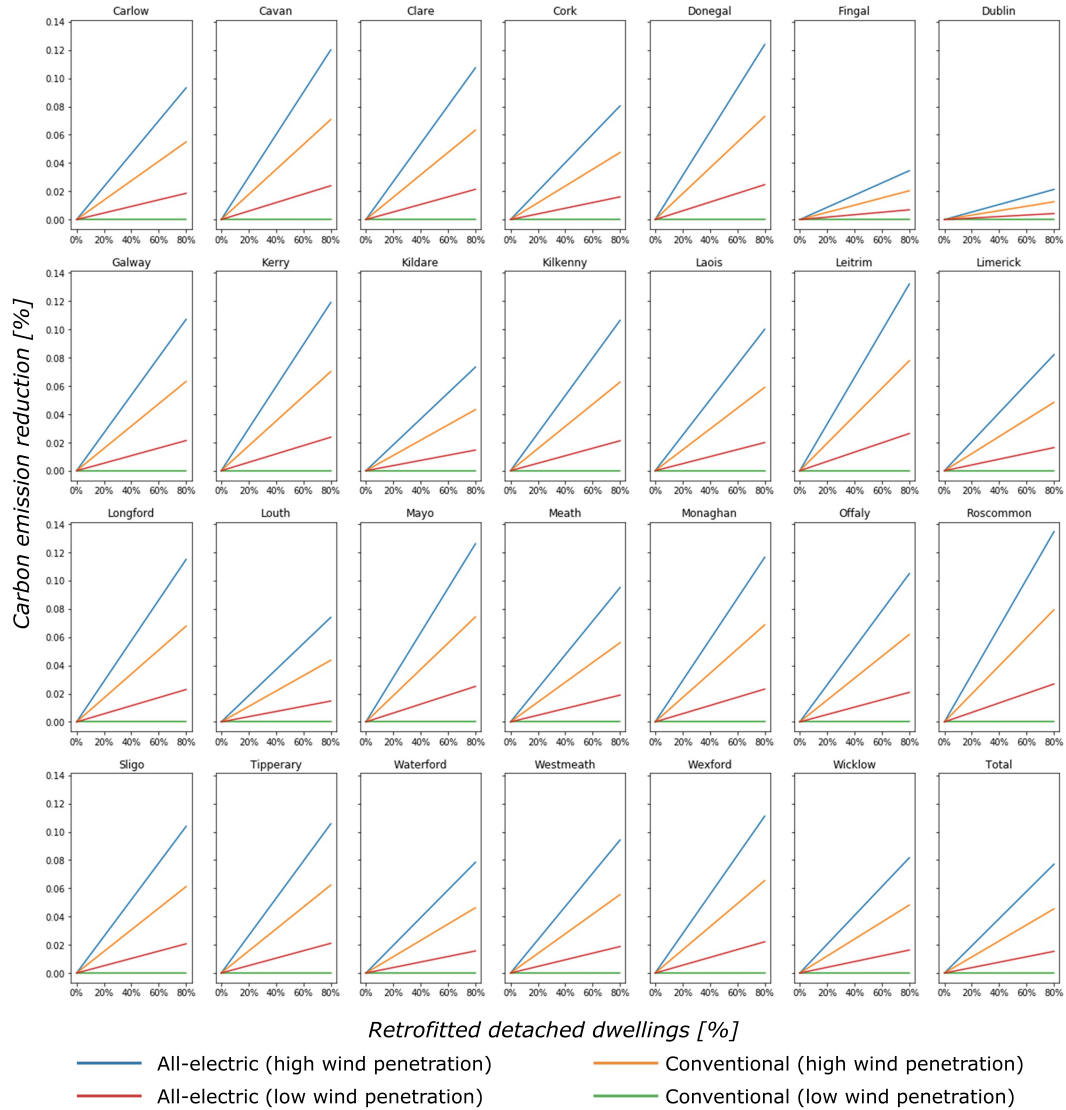


Figure 12.: Carbon emissions reduction for different percentages of retrofitted detached houses (20-40-60-80) and different RES penetration scenarios. Note: Dublin county is subdivided into two groups: Fingal and Dublin (South Dublin, Dun Laoghaire/Rathdown and Dublin City).

all electric equipment, including a PV and a GSHP systems. Moreover, an electric vehicle, charged via the household electricity supply, replaced a conventional gasoline automobile. The retrofit measures installed in the building were representative of specific measures that are likely to be adopted by many future new residential building developments.

Following the retrofit phase, the building was equipped with a HAN consisting of approximately 30 sensors with a 15 minute monitoring resolution. The experimental data collected during the experimental campaign was used to calibrate an EnergyPlus model of the dwelling. Specific metrics (i.e., MBE and CVRMSE) were introduced to assess the accuracy of each subsystem model to predict the energy consumption. The objective of developing an accurate calibrated building model using measured data

was to test and analyse the impact of retrofit measures on the building consumption and on associated carbon emissions.

The results of the calibration procedure showed that the EnergyPlus model was capable of reproducing the building electricity consumption with an overall accuracy of $MBE = -1.6\%$ and $CVRMSE = 10\%$. Specifically, the calibration of the GSHP model was within the ASHRAE thresholds, with values of MBE and CVRSMSE equal to 3.78% and -0.61%, respectively. Moreover, a satisfactory match between experimental and numerical results were obtained for the PV system, (MBE and CVRMSE of 3.6% and 12.5%, respectively) and the electric vehicle (MBE and CVRMSE of 3.5% and 10.4%, respectively). Since the activity patterns of the occupants were not tracked for privacy reasons, the calibration of the thermal envelope was performed on five selected days when the occupants were not in the building, showing MBE and CVRMSE values below the hourly ASHRAE standard.

Post calibration, the resulting EnergyPlus model was used to investigate the effectiveness of the implemented retrofitting measures in terms of energy savings and carbon emissions reduction. The results showed a 45% increment the overall building energy performance of the retrofitted building (i.e., all-electric scenario) compared to the pre-retrofitted building (no retrofitting). Moreover, data from the Irish system operator was used to calculate the carbon footprint of the building. A carbon emissions reduction of approximately 28.9% was obtained by the retrofitted all-electric building compared to the pre-retrofitted one.

Finally, the impact of the retrofitting measures in terms of carbon dioxide emissions for two different scenarios of wind penetration (high and low wind power generation) was carried out. Generally, the retrofitted all-electric building always displayed a reduction in the carbon emissions compared to the pre-retrofitted building, which ranged from 4% to 18%, for the low wind and high wind penetration scenarios, respectively. Furthermore, the analysis was extended to a country level by considering different penetration scenarios of the retrofitting (all-electric) measures for one subset (detached dwellings) of the Irish building stock. Since the distribution of the building archetypes in Ireland is not uniform on a geographical spatial basis, the investigation was performed at county level to highlight potential non-homogeneity. Results showed that implementing the retrofitting measures at scale could lead to a carbon emissions reduction under high renewable energy penetration scenarios up to 14% for rural areas, while higher density areas exhibit lower benefits. Therefore, targeted policies at a county level, together with a concerted deployment of smart grid infrastructure and RES to smooth grid instability and congestion, could increase the overall effectiveness of retrofit measures.

Disclosure statement

No potential conflict of interest was reported by the authors.

Acknowledgements

This work was conducted at the Electricity Research Centre, University College Dublin, Ireland, which is supported by the Commission for Energy Regulation, Bord Gais Energy, Bord na Mona, Cylon Controls, EirGrid, Electric Ireland, Energia, EPRI, ESB International, ESB Networks, Gaelectric, Intel, SSE Renewables, and UTRC.

This publication has emanated from research conducted with the financial support of PRLTI[R12681]. The authors would like to thank the building owners for their essential support.

References

- Allesina, G., Mussatti, E., Ferrari, F., & Muscio, A. (2018). A calibration methodology for building dynamic models based on data collected through survey and billings. *Energy and Buildings*, 158, 406–416.
- ASHRAE. (2002). Measurement of energy and demand savings. , 17. (ASHRAE Guideline 14-2002)
- Atam, E. (2017). Current software barriers to advanced model-based control design for energy-efficient buildings. *Renewable and Sustainable Energy Reviews*, 73, 1031–1040.
- Buildings Performance Institute Europe. (2014). *Data hub for energy performance of buildings*. [online resource]. Retrieved from <https://www.buildingsdata.eu>
- Carragher, M., De Rosa, M., Kathirgamanathan, A., & Finn, D. P. (2019). Investment analysis of gas-turbine combined heat and power systems for commercial buildings under different climatic and market scenarios. *Energy Conversion and Management*, 183, 35 - 49.
- Castaldo, V., Coccia, V., Cotana, F., Pignatta, G., Pisello, A., & Rossi, F. (2015). Thermal-energy analysis of natural cool stone aggregates as passive cooling and global warming mitigation technique. *Urban Climate*, 14, 301–314.
- Clauß, J., Vogler-Finck, P., & Georges, L. (2018). Calibration of a high-resolution dynamic model for detailed investigation of the energy flexibility of a zero emission residential building. In *Cold climate hvac conference* (pp. 725–736).
- Coakley, D. (2014). *Calibration of detailed building energy simulation models to measured data using uncertainty analysis*. (PhD dissertation. NUI Galway)
- Coakley, D., Raftery, P., & Keane, M. (2014). A review of methods to match building energy simulation models to measured data. *Renewable and Sustainable Energy Reviews*, 37, 12–41.
- Commission for Energy Regulation. (2011). *Smart metering cost-benefit analysis and trials findings reports*. Retrieved from <https://mk0cruiefjep6wj7niq.kinstacdn.com/wp-content/uploads/2011/07/cer11080c.pdf>
- Commission for Energy Regulation. (2013). *Ds3 - system services technical definitions*. Retrieved from <https://www.semcommittee.com/news-centre/ds3-system-services-technical-definitions-decision-paper>
- De Rosa, M., Bianco, V., Scarpa, F., & Tagliafico, L. A. (2016). Impact of wall discretization on the modeling of heating/cooling energy consumption of residential buildings. *Energy Efficiency*, 9(1), 95–108.
- D’Ettorre, F., De Rosa, M., Conti, P., Testi, D., & Finn, D. (2019). Mapping the energy flexibility potential of single buildings equipped with optimally-controlled heat pump, gas boilers and thermal storage. *Sustainable Cities and Society*, 50, 101689.
- Dimitroulopoulou, C. (2012). Ventilation in european dwellings: A review. *Building and Environment*, 47, 10-25. (International Workshop on Ventilation, Comfort, and Health in Transport Vehicles)
- Eirgrid. (2015). *Co2 intensity & emissions: All island*. online. Retrieved from <http://smartgriddashboard.eirgrid.com/>
- Ellis, P. G., Torcellini, P. A., & Crawley, D. B. (2008). *Simulation of energy management systems in energyplus*. National Renewable Energy Laboratory.
- EnergyPlus Engineering Reference. (2015). *Engineering reference manual* (Tech. Rep.). U.S. Department of Energy. Retrieved from https://energyplus.net/sites/default/files/pdfs_v8.3.0/EngineeringReference.pdf
- EnergyTrust. (2005). *Improving air tightness in dwellings*. Retrieved from <http://www>

- .berireland.ie/BER.technical.html (CE137/GPG224)
- European Union. (2012). *Directive 2012/27/eu of the european parliament and of the council of 25 october 2012 on energy efficiency, amending directives 2009/125/ec and 2010/30/eu and repealing directives 2004/8/ec and 2006/32/ec.* (Official Journal of the European Union.)
- European Union. (2016). An eu strategy on heating and cooling. *Communication from the Commission to the European Parliament, the Council, the European Economic and Social Committee and the Committee of the Regions.* Retrieved from https://ec.europa.eu/energy/sites/ener/files/documents/1.EN_ACT_part1_v14.pdf
- European Union. (2018). *Directive (eu) 2018/844 of the european parliament and of the council of 30 may 2018 amending directive 2010/31/eu on the energy performance of buildings and directive 2012/27/eu on energy efficiency.* (Official Journal of the European Union.)
- Fabrizio, E., & Monetti, V. (2015). Methodologies and advancements in the calibration of building energy models. *Energies*, 8(4), 2548–2574.
- Glasgo, B., Hendrickson, C., & Azevedo, I. L. (2017). Assessing the value of information in residential building simulation: Comparing simulated and actual building loads at the circuit level. *Applied Energy*, 203, 348 - 363.
- Goy, S., Ashouri, A., Maréchal, F., & Finn, D. (2017). Estimating the potential for thermal load management in buildings at a large scale: Overcoming challenges towards a replicable methodology. *Energy Procedia*, 111, 740 - 749.
- Haves, P., Salsbury, T., Claridge, D., & Liu, M. (2001). *Use of whole building simulation in on-line performance assessment: Modeling and implementation issues* (Tech. Rep.). Ernest Orlando Lawrence Berkeley National Lab., CA (US).
- Hopfe, C. J., & Hensen, J. L. (2011). Uncertainty analysis in building performance simulation for design support. *Energy and Buildings*, 43(10), 279-805.
- INES. (2013). *Nissan leaf charging profile* (Tech. Rep.). National Solar Energy Institute, Grenoble, France.
- Ireland Central Statistics Office. (2012). *The roof over our heads.* Retrieved from <http://www.cso.ie>
- Irish Central Statistics Office. (2016). *Census of population 2016 - housing in ireland.* [online resource]. Retrieved from <https://www.cso.ie>
- Irish Government. (2011). *Building regulation 2011 - technical guidance document 1. conservation of fuel and energy - dwellings* (Tech. Rep.). Retrieved from <https://www.housing.gov.ie/sites/default/files/migrated-files/en/Publications/DevelopmentandHousing/BuildingStandards/FileDownload%2C27316%2Cen.pdf>
- Kalogirou, S. A. (2004). Solar thermal collectors and applications. *Progress in energy and combustion science*, 30(3), 231–295.
- Keiser, G. (1989). *Local area networks.* McGraw-Hill New York.
- Leal, V. M., Granadeiro, V., Azevedo, I., & Boemi, S.-N. (2015). Energy and economic analysis of building retrofit and energy offset scenarios for net zero energy buildings. *Advances in Building Energy Research*, 9(1), 120–139.
- Li, W., Tian, Z., Lu, Y., & Fu, F. (2018). Stepwise calibration for residential building thermal performance model using hourly heat consumption data. *Energy and Buildings*, 181, 10 - 25.
- Ma, Z., Cooper, P., Daly, D., & Ledo, L. (2012). Existing building retrofits: Methodology and state-of-the-art. *Energy and buildings*, 55, 889–902.
- Marra, F., Yang, G. Y., Traholt, C., Larsen, E., Rasmussen, C. N., & You, S. (2012). Demand profile study of battery electric vehicle under different charging options. In *Power and energy society general meeting, 2012 IEEE* (pp. 1–7).
- Masoum, A. S., Deilami, S., Moses, P. S., & Abu-Siada, A. (2010, Oct). Impacts of battery charging rates of plug-in electric vehicle on smart grid distribution systems. In *2010 IEEE PES innovative smart grid technologies conference europe (ISGT Europe)* (p. 1-6).
- Mata, É., Kalagasidis, A. S., & Johnsson, F. (2014). Building-stock aggregation through archetype buildings: France, germany, spain and the uk. *Building and Environment*, 81, 270–282.

- Mauro, G. M., Hamdy, M., Vanoli, G. P., Bianco, N., & Hensen, J. L. (2015). A new methodology for investigating the cost-optimality of energy retrofitting a building category. *Energy and Buildings*, *107*, 456–478.
- McGinnity, F., Russel, H., Williams, J., & Blackwell, S. (2005). *Time-use in ireland 2005: Survey dataset*. The Economic and Social Research Institute, Dublin. Ireland.
- Modbus, I. (2004). Modbus application protocol specification v1. 1a. *North Grafton, Massachusetts*.
- Mustafaraj, G., Marini, D., Costa, A., & Keane, M. (2014). Model calibration for building energy efficiency simulation. *Applied Energy*, *130*, 7-5.
- Neu, O., Oxizidis, S., Flynn, D., Pallonetto, F., & Finn, D. (2013). High resolution space-time data: methodology for residential building simulation modelling. *IPBSA*.
- NextGreenCar. (2016). *Zap map - ev trip planner*. Online. Retrieved from <https://www.zap-map.com/>
- Oller, P. E., Rodríguez, J. M. A., González, Á. S., Fariña, E. A., & Álvarez, E. G. (2018). Improving the calibration of building simulation with interpolated weather datasets. *Renewable energy*, *122*, 608–618.
- Pallonetto, F., De Rosa, M., Milano, F., & Finn, D. P. (2019). Demand response algorithms for smart-grid ready residential buildings using machine learning models. *Applied Energy*, *239*, 1265 - 1282.
- Pallonetto, F., Mangina, E., Finn, D., Wang, F., & Wang, A. (2014). A restful api to control a energy plus smart grid-ready residential building: demo abstract. In *Proceedings of the 1st acm conference on embedded systems for energy-efficient buildings* (pp. 180–181).
- Pallonetto, F., Mangina, E., Milano, F., & Finn, D. P. (2019). Simapi, a smartgrid co-simulation software platform for benchmarking building control algorithms. *SoftwareX*, *9*, 271–281.
- Raftery, P. (2011). *Calibrated whole building energy simulation: An evidence-based methodology*. (PhD dissertation. NUI Galway.)
- Reddy, T. A., Maor, I., & Panjapornpon, C. (2007). Calibrating detailed building energy simulation programs with measured data, part i: General methodology (rp-1051). *Hvac&R Research*, *13*(2), 221–241.
- Rey, E. (2004). Office building retrofitting strategies: multicriteria approach of an architectural and technical issue. *Energy and Buildings*, *36*(4), 367–372.
- Rogelj, J., Den Elzen, M., Höhne, N., Fransen, T., Fekete, H., Winkler, H., ... Meinshausen, M. (2016). Paris agreement climate proposals need a boost to keep warming well below 2 c. *Nature*, *534*(7609), 631–639.
- Royapoor, M., & Roskilly, T. (2015). Building model calibration using energy and environmental data. *Energy and Buildings*, *94*, 109–120.
- SEAI. (2011a, 10). *Residential energy road map*. Online. Retrieved from http://www.seai.ie/Renewables/Residential\Energy_Roadmap.pdf
- SEAI. (2011b, 10). *Smart grid road map*. Online. Retrieved from http://www.seai.ie/Publications/Statistics_Publications/SEAI_2050_Energy_Roadmaps/Smartgrid.Roadmap.pdf
- SEAI. (2012). *Sustainable energy authority of ireland: Emission factors from different fuels*. (http://www.seai.ie/Publications/Statistics_Publications/EmissionFactors/)
- SEAI. (2013). *Energy in the residential sector*. Retrieved from http://www.seai.ie/Publications/Statistics_Publications/Energy-in-the-Residential-Sector/Energy-in-the-Residential-Sector-2013.pdf
- SEAI. (2017). *Sustainable energy authority of ireland: Domestic fuels*. (empty)
- Shin, Y. H., Sim, S., & Kim, S. C. (2016). Performance characteristics of a modularized and integrated ptc heating system for an electric vehicle. *Energies*, *9*(1). Retrieved from <http://www.mdpi.com/1996-1073/9/1/18>
- Single Electricity Market Committee. (2011). *Demand side vision for 2020*. Retrieved from <https://www.semcommittee.com/news-centre/demand-side-vision-2020>
- Sinnott, D., & Dyer, M. (2012). Air-tightness field data for dwellings in ireland. *Building and*

- Environment*, 51, 269–275.
- Smith, W. J. (2010). Can ev (electric vehicles) address ireland carbon emissions from transport? *Energy*, 35(12), 4514–4521.
- Szalay, Z., & Csoknyai, T. (2014). The road to nearly zero-energy buildings. *International Journal for Housing Science & Its Applications*, 38(4).
- Thomsen, K. E., Rose, J., Mørck, O., Jensen, S. Ø., Østergaard, I., Knudsen, H. N., & Bergsøe, N. C. (2016). *Energy and Buildings*, 123, 8–16.
- Vázquez-Canteli, J. R., & Nagy, Z. (2019). Reinforcement learning for demand response: A review of algorithms and modeling techniques. *Applied energy*, 235, 1072–1089.
- Westphal, F. S., & Lamberts, R. (2005). Building simulation calibration using sensitivity analysis. In *In proceedings of ninth international ibpsa conference*.
- Yi, P., Iwayemi, A., & Zhou, C. (2010). Developing zigbee deployment guideline under wifi interference for smart grid applications. *IEEE transactions on smart grid*, 2(1), 110–120.
- Yin, R., Kiliccote, S., & Piette, M. A. (2016). Linking measurements and models in commercial buildings: A case study for model calibration and demand response strategy evaluation. *Energy and Buildings*, 124, 222 - 235.